Site and Orbit Repeatability using Adaptive Mapping Functions

Camille Desjardins [(1)], Pascal Gegout [(2)], Laurent Soudarin [(3)], Richard Biancale [(4)], Felix Perosanz [(4)]
(1) CNES/CLS/GRGS (Camille.Desjardins@cnes.fr), (2) CNRS/GET/GRGS, Géosciences Environnement Toulouse (Pascal.Gegout@get.omp.eu), (3) Collecte Localisation Satellite, Ramonville St-Agne, (4) CNES/GRGS, France

1 – Introduction

The electromagnetic signals emitted by the satellite positioning systems travel at the speed of light in a straight line in a vacuum but are modified in their propagation through the neutral atmosphere by temporal and spatial changes of density, composition and refractivity. These waves are slowed down and their trajectories are bent.

This presentation summarizes the performances of the modeling of the tropospheric propagation by the ray tracing technique through the assimilations of the European Meteorological Centre (ECMWF) in the framework of realizing the geodetic reference frame. This goal is achieved by modeling the spatial variability of the propagation using the time variable three-dimensional physical parameters of the atmosphere.
The tropospheric delays, obtained by tracing rays in all directions throughout the meteorological model surrounding the geodetic site (Desjardins et al., 2015; Gegout et al., 2014), are fitted by Adaptive Mapping Functions (AMF defined by Gegout et al., 2011) parameterized by several tens of coefficients.
The delays produced by the Horizon software are then tested, kept unchanged or adjusted, when recovering a reference frame based on hundred sites using the GINS software.

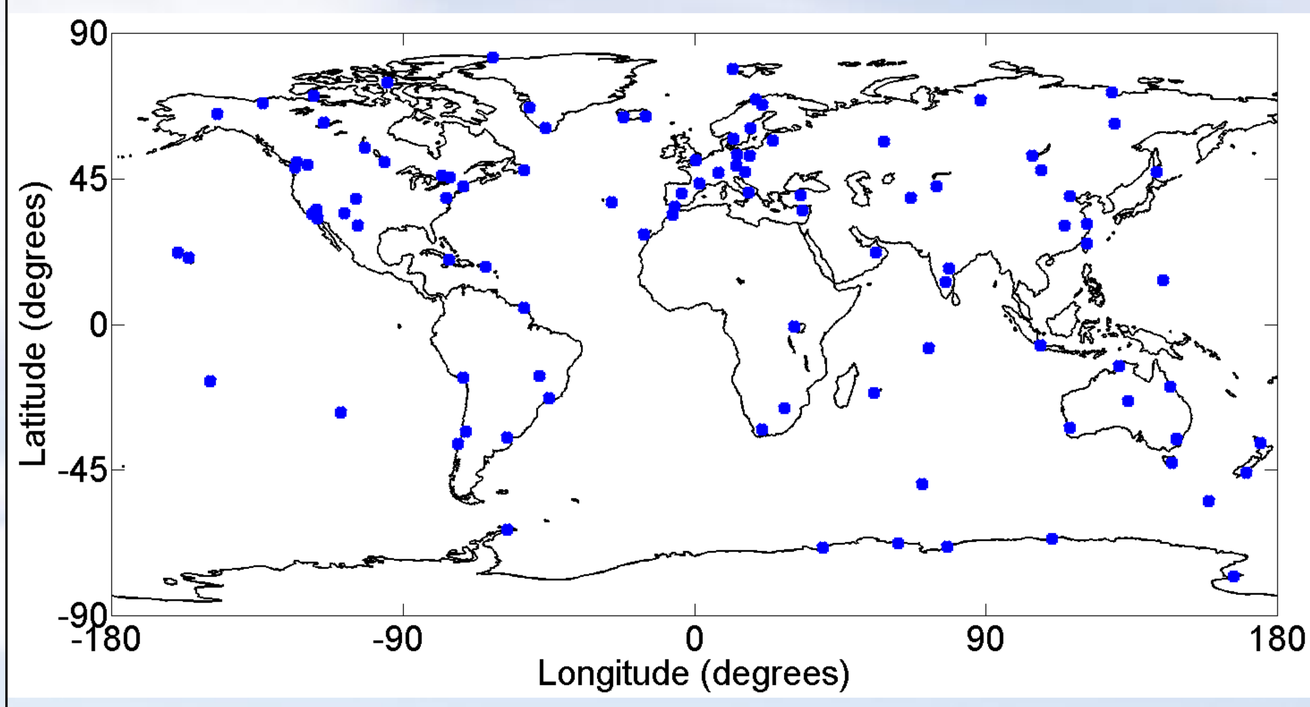

Code	Site Name, Country	λ (°)	φ (°)	h (m)
MCM4	Ross Island, Antarctica	166.6693	-77.8383	98.0222
SYOG	East Ongle Island, Antarctica	39.5837	-69.0070	50.0902
DAV1	Davis, Antarctica	77.9726	-68.5773	44.5000
MAW1	Mawson, Antarctica	62.8707	-67.6048	59.1840
CAS1	Casey, Antarctica	110.5197	-66.2834	22.5500
OHI3	O'Higgins, Antarctica	302.0986	-63.3211	32.1500
MAC1	MacQuarie Island, Southern Ocean	158.9358	-54.4995	-6.6900
KERG	Port aux Franais, Kerguelen Islands	70.2555	-49.3515	74.0583
OUS2	Dunedin, New Zealand	170.5109	-45.8695	26.1000
HOB2	Hobart, Australia	147.4387	-42.8047	41.1270
CONZ	Concepcion, Chile	286.9745	-36.8438	181.2000
AUCK	Whangaparaoa Peninsula, New Zealand	174.8344	-36.6028	132.7110
TIDB	Tidbinbilla, Australia	148.9800	-35.3992	665.3719
STR1	Canberra, Australia	149.0109	-35.3155	800.0320
LPGS	La Plata, Argentina	302.0677	-34.9067	29.9000
SANT	Santiago, Chile	289.3314	-33.1503	723.0746
SUTH	Sutherland, South Africa	20.8105	-32.3802	1799.7659
PERT	Perth, Australia	115.8852	-31.8019	12.9200
ISPA	Easter Island, Chile	250.6556	-27.1250	112.4948
HARB	Pretoria, South Africa	27.7075	-25.8869	1555.0000
ALIC	Alice Springs, Australia	133.8855	-23.6701	603.3581
CHPI	Cachoeira Paulista, Brazil	315.0148	-22.6871	617.4176
REUN	Le Tampon, France	55.5717	-21.2083	1558.4000
TOW2	Cape Ferguson, Australia	147.0557	-19.2693	88.2349
THTI	Papeete, French Polynesia	210.3937	-17.5769	98.0400
AREQ	Arequipa, Peru	288.5072	-16.4655	2488.9226
BRAZ	Brasilia, Brazil	312.1222	-15.9474	1106.0413
DARW	Darwin, Australia	131.1327	-12.8437	125.1965
DGAR	Diego Garcia Island, U.K.	72.3702	-7.2697	-64.7455
BAKO	Cibinong, Indonesia	106.8500	-6.4900	158.1800
MBAR	Mbarara, Uganda	30.7379	-0.6015	1337.6533
KOUR	Kourou, French Guiana	307.1940	5.2522	-25.5700
IISC	Bangalore, India	77.5704	13.0212	843.7145
GUAM	Dededo, Guam	144.8683	13.5893	201.9220
HYDE	Hyderabad, India	78.5509	17.4173	441.6800
CRO1	Christiansted, Virgin Islands, U.S.	295.4157	17.7569	-31.9558
SCUB	Santiago de Cuba, Cuba	284.2377	20.0121	21.9000
MAUI	Haleakala, Maui, U.S.	203.7430	20.7067	3062.0000
KOKB	Kokee Park, Waimea, U.S.	200.3351	22.1263	1167.5216
YIBL	Yibal, Oman	56.1123	22.1865	95.1000
TWTF	Taoyuan, Republic of China	121.1645	24.9536	203.1220
MAS1	Maspalomas, Spain	344.3667	27.7637	197.3000
WUHN	Wuhan, P.R. China	114.3573	30.5317	28.2000
MDO1	Fort Davis, U.S.	255.9850	30.6805	2004.4761
SHAO	Sheshan, China	121.2004	31.0996	22.0901
MONP	Laguna Mountains, U.S.	243.5800	32.8900	1842.5500
RABT	Rabat, Morocco	353.1457	33.9981	90.1000
JPLM	Pasadena, U.S.	241.8268	34.2048	423.9843
PIE1	Pie Town, U.S.	251.8811	34.3015	2347.7109
NICO	Nicosia, Cyprus	33.3964	35.1409	155.0000
GOLD	Goldstone, U.S.	243.1107	35.4252	986.6779
SFER	San Fernando, Spain	353.7944	36.4643	85.8000
PDEL	Ponta Delgada, Portugal	334.3372	37.7477	110.8000
AMC2	Colorado Springs, U.S.	255.4754	38.8031	1912.4898
GODE	Greenbelt, U.S.	283.1732	39.0217	14.5046
KIT3	Kitab, Uzbekistan	66.8800	39.1400	643.0000
BJFS	Fangshan, China	115.8925	39.6086	87.4130
ANKR	Ankara, Turkey	32.7586	39.8875	974.8000
VILL	Villafranca, Spain	356.0480	40.4436	647.5000
MATE	Matera, Italy	16.7045	40.6491	535.6000
WES2	Westford, U.S.	288.5067	42.6133	85.0000
POL2	Bishkek, Kyrghyzstan	74.6943	42.6798	1714.2000
TLSE	Toulouse, France	1.4809	43.5607	207.2000
NRC1	Ottawa, Canada	284.3762	45.4542	82.5000
ALGO	Algonquin Park, Canada	281.9286	45.9588	202.0000
ZIMM	Zimmerwald, Switzerland	7.4653	46.8771	956.7000
YSSK	Yuzhno-Sakhalinsk, Russia	142.7167	47.0297	91.2887
GRAZ	Graz, Austria	15.4935	47.0671	538.3000
STJO	St. John's, Canada	307.3223	47.5952	152.8000
ULAB	Ulaanbataar, Mongolia	107.0500	47.6700	1611.7000
ALBH	Victoria, Canada	236.5126	48.3898	32.0000
WTZZ	Bad Koetzting, Germany	12.8789	49.1442	665.8900
DRAO	Penticton, Canada	240.3750	49.3226	542.0000
WSLR	Whistler, Canada	237.0788	50.1265	909.0000
DUBO	Lac du Bonnet, Canada	264.1338	50.2588	251.0000
HERS	Hailsham, U.K.	0.3362	50.8673	76.5000
HERT	Hailsham, U.K.	0.3344	50.8675	83.3000
BOR1	Borowiec, Poland	17.0668	52.1002	124.0000
IRKJ	Irkutsk, Russia	104.3162	52.2190	502.1000
POTS	Potsdam, Germany	13.0661	52.3793	174.0000
FLIN	CFS FLIN FLON, Canada	258.0220	54.7256	320.0000
ARTU	Arti, Russia	58.5605	56.4298	247.5110
RIGA	Riga, Latvia	24.0587	56.9486	34.7000
ONSA	Onsala, Sweden	11.9255	57.3953	45.5000
MAR6	Maartsbo, Sweden	17.2585	60.5951	75.4000
QAQ1	Qaqortoq / Julianehaab, Greenland	313.9522	60.7152	110.4000
YAKT	Yakutsk, Russia	129.6803	62.0310	103.3700
YELL	Yellowknife, Canada	245.5193	62.4809	181.0000
REYK	Reykjavik, Iceland	338.0445	64.1388	93.1000
HOFN	Hoefn, Iceland	344.8132	64.2673	82.5000
FAIR	Fairbanks, U.S.	212.5008	64.9780	319.1771
KELY	Kangerlussuaq, Greenland	309.0552	66.9874	229.8000
KIRU	Kiruna, Sweden	20.9684	67.8573	391.1000
INVK	Inuvik, Canada	226.4730	68.3062	46.3600
NRIL	Norilsk, Russia	88.3598	69.3618	47.8937
TRO1	Tromsoe, Norway	18.9396	69.6627	138.0000
HOLM	Ukhkhaktok, Victoria Island, Canada	242.2391	70.7364	39.5000
TIXI	Tixi, Russia	128.8664	71.6345	46.9847
RESO	Resolute, Cornwallis Island, Canada	265.1067	74.6908	34.9000
NYAL	Ny-Alesund, Norway	11.8700	78.9300	82.0000
ALRT	Alert, Ellesmere Island, Canada	297.6595	82.4943	78.1100

Table 1: Coordinates of the 100 GPS sites, sorted by ascending latitude, from South Pole to North Pole. The sites on all graphs follow this order.

2 – Methodology and Results

The method for determining GPS orbits and sites positions is the methodology defined by the CNES/CLS Analysis Center for the IGS campaign REPRO2 and ITRF 2014 (Loyer et al., 2012). Estimated parameters are the position and speed of the GPS satellites, the parameters of the solar radiation pressure and the biases of satellites and sites clocks.

The standard approach for mitigating tropospheric delays use the GPT2 empirical model associated to the Vienna Mapping Function VMF1 (Boehm et al., 2006). The custom approach is the use of Adaptive Mapping Functions. The experiments are defined in the table 2 on the right. RMS of phase residuals are provided below as a measure of the AMF model performance.

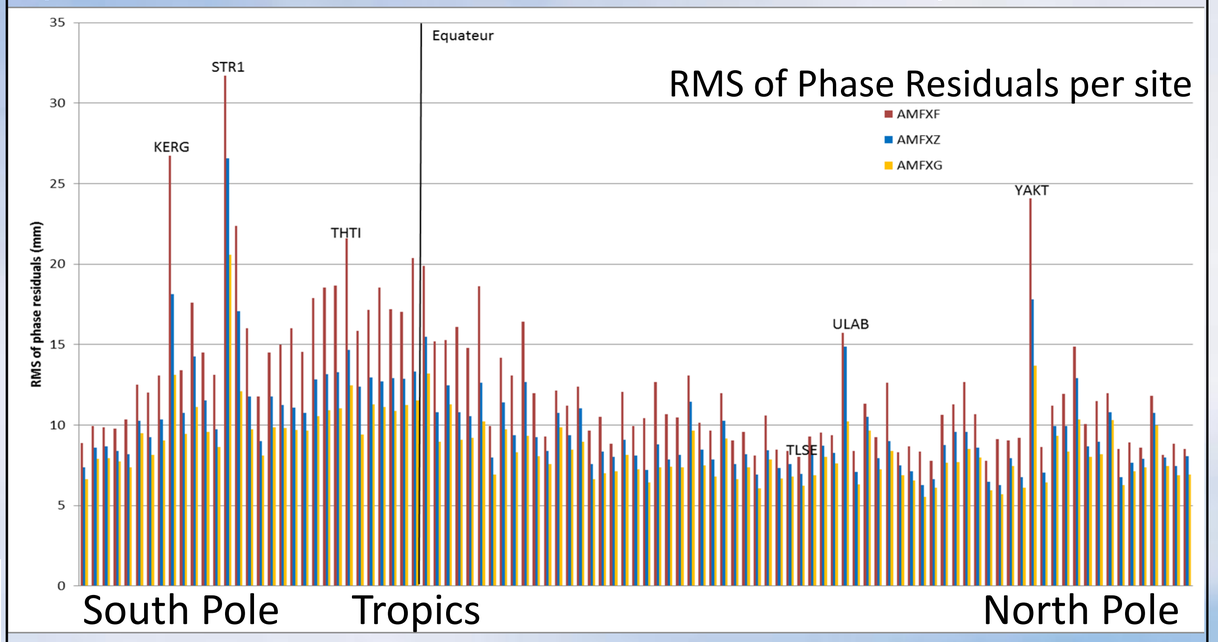

The RMS of phase residuals is obtained for each site at the measurement level from all GPS measures of February 2013. The AMFXF experiment shows RMS from 10±3 mm at mid- and high-latitudes. RMS reach 15 to 20 mm near the Equator. The zenithal delay is adjusted in the AMFXZ experiment: phase residuals decrease in the tropics where humidity is known to fluctuate rapidly. Optimal delays differ from snapshot delays. The AMFXG experiment with adjusted gradients improve the phase residuals by several millimeters. RMS of phase residuals 10±2 mm in the tropics and 8±2 mm at mid and high-latitudes.

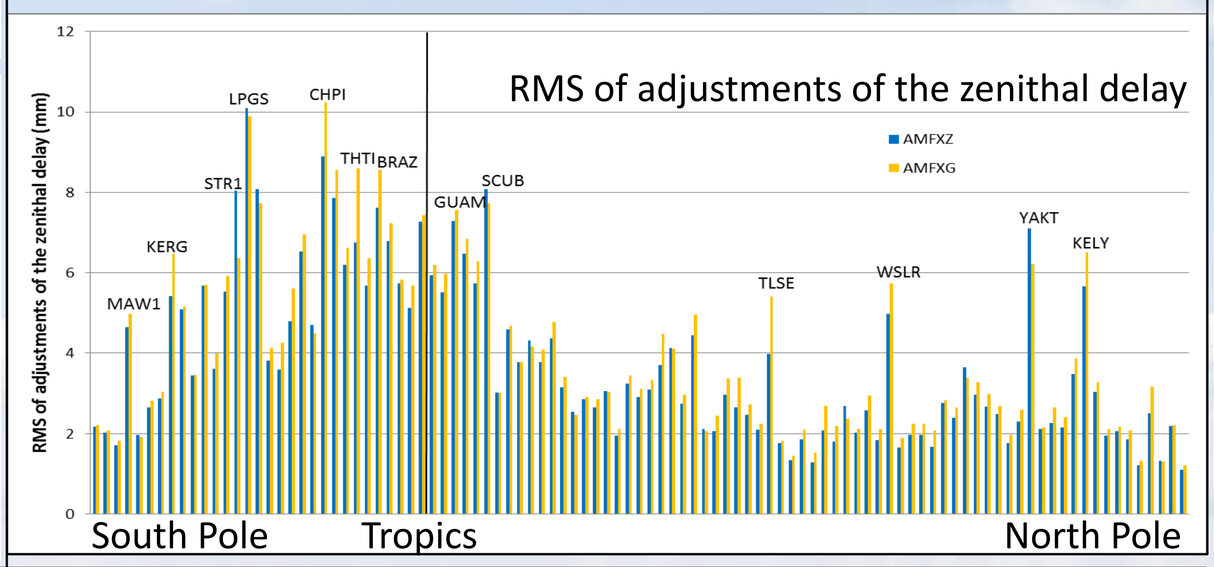

The zenithal delay adjustments are geographically correlated with areas of rapidly changing humidity. Even if not adjusted, AMFs already provide low phase residuals. The adjustments compensate rapidly changing humidity which is not well sampled by 3-hourly assimilation snapshots. In areas of large asymmetric distribution of humidity, e.g. land/ocean contrast in the tropics, adjusting horizontal gradients fits better.

3 – Orbit Repeatability, Phase Residuals and Resolved Integer Ambiguity

Several experiments summarized in the table 2 below were realized: the models were kept unmodified (GPTGF, AMFXF), the zenith delay (GPTGZ, AMFXZ) and additionally gradients (GPTGG, AMFXG) thanks to the mapping function formalism, were **simultaneously adjusted at the observation level** to all parameters: GPS orbits, 100 sites, clocks, ambiguities, ...

When zenith delays or zenith delays and gradients are adjusted with all other parameters, orbit repeatability, phase residuals and solved integer ambiguities indicates that AMF and GPT2+VMF1 provide solutions with the same accuracy. The AMFXF model, even if all AMF parameters are kept fixed, already provides reliable orbits and clocks solutions.

Table 2 Model	Experiment	Adjusted Parameters	Orbit Repeatability RMS (cm)	Phase residuals RMS (mm)	Resolved Integer Ambiguity (%)
GPT2+ VMF1	GPTGF	all parameters fixed	246.22	72.83	-
	GPTGZ	Zenith delay	3.51	10.54	94.95
	GPTGG	Zenith delay + Gradients	3.39	8.87	97.14
AMF	AMFXF	all parameters fixed	4.24	13.16	94.45
	AMFXZ	Zenith delay	3.49	10.34	95.29
	AMFXG	Zenith delay + Gradients	3.36	8.83	96.66

4 – Site Repeatability In the vertical direction

When the zenith delay and gradients are adjusted, the repeatability of the vertical position is not enhanced by changing the model of propagation. This limit may also be due to the lack or deficiency of other models, such as non-tidal and tidal loading, known to impact the height, the vertical component, of sites at the centimeter level.

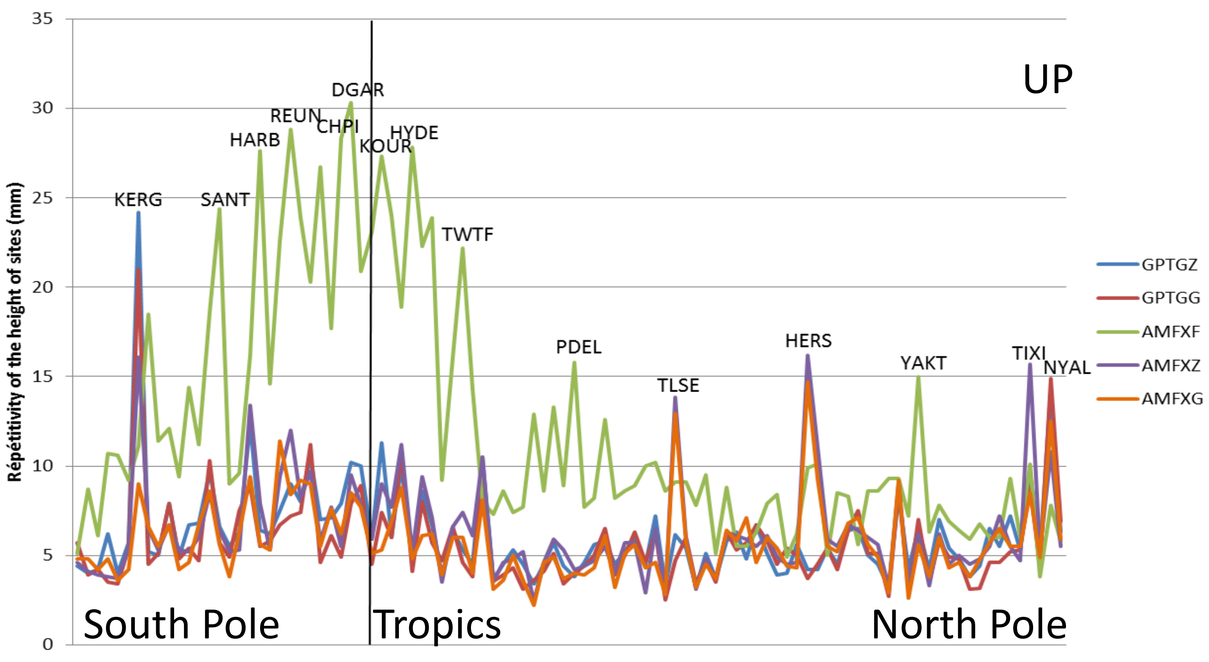

5 – Site Repeatability In the horizontal directions

At the contrary, the repeatability of the horizontal position of geodetic sites is greatly enhanced by accounting for the azimuthal variability provided by the realistic shapes of the Atmosphere and the Earth. The rigorous interpolations of atmospheric physical parameters and the realistic anisotropy included in Adaptive Mapping Functions lead to this result.

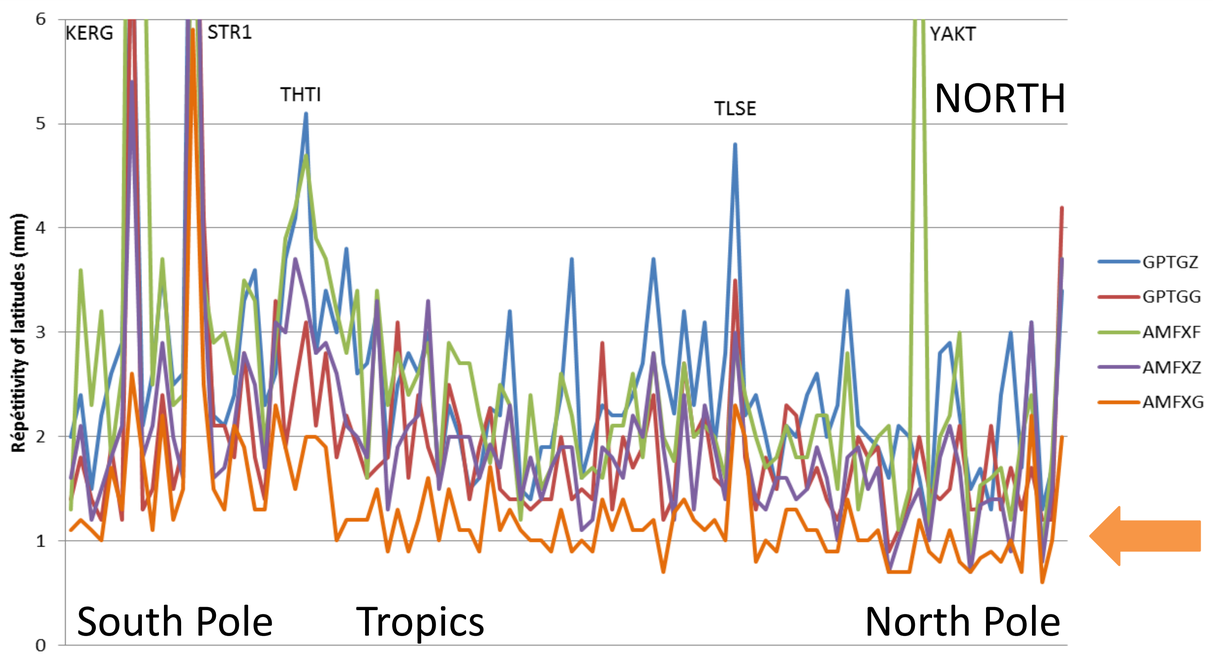

6 – Mean Repeatability (all sites)

Table 3 Experiment	Adjusted Parameters	Latitudes (mm)	Longitudes (mm)	Heights (mm)
GPTGZ	Zenith delay	2.58	2.19	6.38
GPTGG	Zenith delay + Gradients	1.98	1.74	5.81
AMFXF	None	2.62	2.32	12.0
AMFXZ	Zenith delay	2.02	1.87	6.20
AMFXG	Zenith delay + Gradients	1.30	1.18	5.70

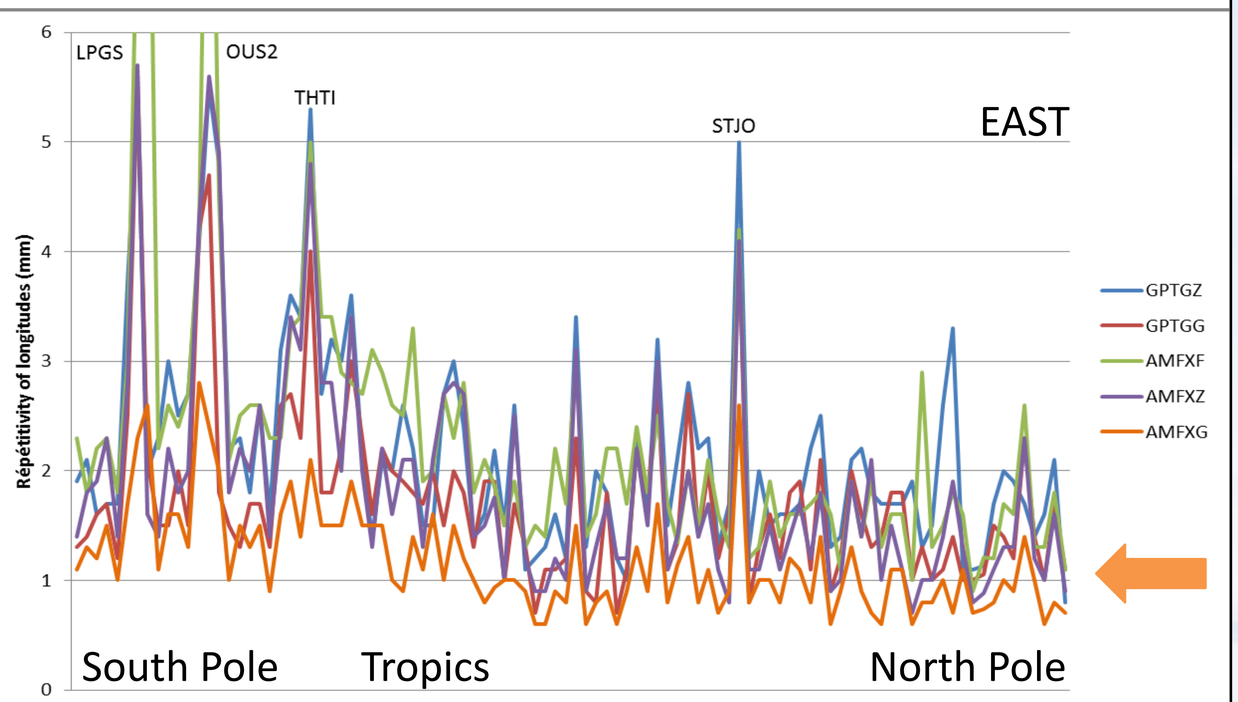

References:

P. Gegout, R. Biancale , L. Soudarin, "**Adaptive Mapping Functions to the Azimuthal Anisotropy of the Neutral-Atmosphere**", *Journal of Geodesy*, Volume 85, Number 10, 661-677, **2011.** http://dx.doi.org/10.1007/s00190-011-0474-y.

S. Loyer, F. Perosanz, F. Mercier, H. Capdeville, J.-C. Marty, "**Zero-difference GPS ambiguity resolution at CNES-CLS IGS Analysis Center**", *Journal of Geodesy*, 86(11) : 991–1003, 2012. ISSN 0949-7714. http://dx.doi.org/10.1007/s00190-012-0559-2

P. Gegout, P. Oberle, C. Desjardins, J. Moyard, P.M. Brunet, "**Ray-tracing of GNSS signal through the atmosphere powered by CUDA, HMPP and GPUs technologies**", *IEEE Journal of Selected Topics in Applied Earth Observations and Remote Sensing*, volume 7, issue 5, pp. 1592-1602, **2014**. doi:10.1109/JSTARS.2013.2272600.

C. Desjardins, P. Gegout, L. Soudarin, R. Biancale, "**Rigorous interpolation of atmospheric state parameters for ray-traced tropospheric delays**", Proceedings of the VIII Hotine-Marussi Symposium, *International Association of Geodesy Symposia*, vol. 142.

Acknowledgements:

The Research & Technology work of Camille Desjardins is supported by CNES and "Collecte Localisation Satellites" (CLS) grants. References, Posters and the Ph.D. thesis by Camille Desjardins are available for download at the following sites : http://gnss.cls.fr/ and http://sdu2e.obs-mip.fr/spip.php?article185 and https://tel.archives-ouvertes.fr/tel-01131181

The European Centre for Medium-range Weather Forecasts (ECMWF) is acknowledged for providing the three-dimensional atmospheric operational model-levels fields of the delayed cutoff data assimilations.

The Research and Development of the HORIZON software based on Adaptive Mapping Functions (AMF) is directed by P. Gegout in the project "Loadings & Propagations" funded by the TOSCA/CNES program.